Numerical Methods for the study of Bose-Einstein Condensates using the Gross-Pitaevskii Equation

Melcior Pijoan, Roger Bahí, Pol Mestres
(Dated: May 31, 2019)

Abstract. The Gross-Pitaevskii equation (GPE) is a mean field approximation used to study Bose-Einstein condensates (BEC). Here, we present a brief derivation of the GPE without the use of second quantization, as well as some of its consequences. Next, we present the implementation in Python of some numerical methods to compute the ground state of BEC. We compare the results with well known theoretical limits and the numerical results obtained using GPELab, a MATLAB toolbox to compute stationary and dynamic solutions of the GPE.

I. INTRODUCTION

The difference between *fermions* and *bosons* is well known from statistical physics: *fermions* cannot occupy the same quantum state (this is known as the Pauli exclusion principle), whereas for *bosons*, any number of them can occupy the same quantum state. When we lower the temperature of a set of bosons, they all tend to occupy the minumum energy state. Therefore, in the limit where the temperature goes to zero, all the particles tend to occupy the same state, and the collection of bosons behaves coherently.

To study such systems from a quantum mechanical point of view, we define a Hamiltonian that takes into account the external potential and the interaction between every pair of particles.

$$\hat{H} = \sum_{i=1}^{N} \big(\frac{p^2}{2m} + V_{ext}(r_i)\big) + \frac{1}{2}\sum_{i=1}^{N}\sum_{i\neq j}^{N} V(|r_i - r_j|)$$

Moreover, we perform the mean-field approximation, which basically assumes that every particle feels a mean-field interaction created by the rest. This implies that, for N particles, the wave function for the BEC can be written as $|\Psi\rangle = |\psi_1\rangle\otimes|\psi_2\rangle ...\otimes|\psi_N\rangle$, assumed to be normalized. Instead of solving the Schrödinger Equation, the method explained by [6] consists in finding the solution by minimizing the free energy $F = E - \mu N = \langle\Psi|\,\hat{H}\,|\Psi\rangle - \mu\,\langle\Psi|\Psi\rangle$. $\langle\Psi|\,\hat{H}\,|\Psi\rangle$ is the sum of three terms:

$$\langle\Psi|\sum_{i=1}^{N}\frac{p^2}{2m}|\Psi\rangle = \sum_{i=1}^{N}\frac{\hbar^2}{2m}\int \nabla\psi^*(r_i)\nabla\psi(r_i) = - N\frac{\hbar^2}{2m}\int \psi^*(r)\nabla^2\psi(r)dr \quad (1)$$

$$\langle\Psi|\sum_{i=0}^{N} V_{ext}(r_i)\,|\Psi\rangle = N\int \psi^*(r)V_{ext}\psi(r)dr \quad (2)$$

$$\langle\Psi|\,\frac{1}{2}\sum_{i=1}^{N}\sum_{i\neq j}V(|r_i - r_j|)\,|\Psi\rangle = \frac{N(N-1)}{2}\int dr\int \psi^*(r')\psi(r)V(|r-r'|)\psi^*(r)\psi(r')dr' \quad (3)$$

$$\mu\,\langle\Psi|\Psi\rangle = \mu\Big(\int \psi^*(r)\psi(r)dr\Big)^N \quad (4)$$

Now, to minimize the free energy we follow the common procedure based on calculus of variations:

$$\frac{\delta F}{\delta\Psi^*} = 0 = N\int[-\frac{\hbar}{2m}\nabla^2\psi(r) + V_{ext}(r)\psi(r) + (N-1)(\int|\psi(r)|^2V(|r-r'|)dr')\psi(r) - \mu\psi(r)]\delta\psi^*(r)dr \quad (5)$$

By assuming an interaction potential due to contact interaction, i.e, $V(|r-r'|) = \frac{4\pi\hbar^2}{m}a\delta(r-r')$, being a the S-wave scattering length, we get the time independent Gross-Pitaevskii equation:

$$-\frac{\hbar^2}{2m}\nabla^2\psi(r) + V_{ext}(r)\psi(r) + N\frac{4\pi\hbar^2}{m}a|\psi(r)|^2\psi(r) = \mu\psi(r) \quad (6)$$

A. Some approximations

The external potential V_{ext} allows us to model the action of the external world on the condensate. Since any potential with a minimum can be locally approximated by a parabola, a harmonic potential is often used: $V_{ext}(r) = \frac{1}{2}m\omega^2r^2$. This is also a fair characterization of the available magnetic traps for alkali atoms [5].

If we neglect the interaction potential we recover a quantum harmonic oscillator, with the well known ground-state solution $\psi(r) \propto e^{-r^2/r_0^2}$ with $r_0 = \sqrt{\frac{2\hbar}{m\omega}}$. In the case where the condensate is dense (N is large), the kinetic energy can be neglected in the so-called Thomas-Fermi approximation and the ground state can be analytically solved to give:

$$\psi(r) = \sqrt{\frac{\mu - m\omega^2r^2/2}{gN}}, \quad \text{where} \quad g = \frac{4\pi\hbar^2}{m}a. \quad (7)$$

B. The time-dependent GPE

The time-dependent GPE is derived from a principle of minimum action, i.e. the action $\int_{t_1}^{t_2}dt\int d^3rL$ shall be minimized. L is the Lagrangian density, defined to be:

$$L = i\frac{\hbar}{2}(\Psi^*\partial_t\Psi - \Psi\partial_t\Psi\partial_t\Psi^*) - \frac{\hbar}{2m}(\nabla\Psi^*)\Delta(\nabla\Psi) - V_{ext}\Psi^*\Psi \quad (8)$$

By using calculus of variations with Ψ of the form $|\Psi\rangle = |\psi\rangle\otimes|\psi\rangle\otimes ...\,|\psi\rangle$ we get the time-dependent Gross-Pitaevskii equation:

$$i\hbar\frac{\partial\Psi}{\partial t} = (-\frac{\hbar^2}{2m}\nabla^2 + V_{ext} + g|\Psi|^2)\Psi \quad (9)$$

II. NUMERICAL METHODS

Starting with the time dependent Gross-Pitaevskii equation we formulate a gradient flow as done in [1] to find the state that minimizes the energy of the system. The time dependent Gross-Pitaevskii equation adding rotation terms is:

$$i\hbar\frac{\partial_t\Psi}{\partial t} = (-\frac{\hbar^2}{2m}\nabla^2 + V + g|\Psi|^2 - \Omega L_z)\Psi \quad (10)$$

This is a Schrödinger equation $i\hbar\partial_t\Psi = \hat{H}\Psi$ with the Hamiltonian $\hat{H} = -\frac{\hbar^2}{2m}\nabla^2 + V + g|\psi|^2 - \Omega L_z$. The energy of the system is $E = \langle\Psi|\,\hat{H}\,|\Psi\rangle$. We make all the variables adimensional following $t \to t/\omega_m$, $x \to xa_0$, $\psi \to \psi/a_0^{3/2}$,$\Omega \to \Omega\omega_m$ with $\omega_m = min(\omega_x, \omega_y, \omega_z)$, $a_0 = \sqrt{\frac{\hbar}{m\omega_m}}$. The adimensional energy, $E_{\beta,\Omega} = \frac{E}{\hbar\omega_m}$ can be calculated as a function of the adimensional variables as

$$E_{\beta,\Omega}(\phi) = \int_{\mathbb{R}^3}\left(\frac{1}{2}|\nabla\phi|^2 + V|\phi|^2 + \frac{\beta}{2}|\phi|^4 - \Omega\phi^* L_z\phi\right)d\mathbf{x}$$

Where $\beta = \frac{4\pi Na}{a_0}$ is the nonlinearity strength that describes the (attractive or repulsive) interactions between atoms within the condensate [7]. We must find the ground state of the system, i.e. the state that minimizes the energy,

$$\phi_g = \underset{\phi\in\mathbb{S}}{argmin}\, E_{\beta,\Omega}(\phi)$$

To solve this problem we use the Continuous Normalized Gradient Flow (CNGF), or "imaginary time" method, as in [1].

$$\begin{cases}\delta_t\phi = -\nabla_{\phi^*}E_{\beta,\Omega} = \frac{1}{2}\Delta\phi - V\phi - \beta|\phi|^2\phi + \Omega L_z\phi\\ \phi(x, t_{n+1}) = \phi(x, t^*_{n+1}) = \frac{\phi(x,t^*_{n+1})}{||\phi(x,t^*_{n+1})||_0}\\ \phi(x,0) = \phi_0(x)\end{cases} \tag{11}$$

The first formula can also be obtained by substituting the time for imaginary time in the original GPE, i.e. $t \to -it$ [4]. The scheme consists in calculating a gradient step, actualize the wave-function with the gradient step and normalize the wave-function.

A. Backward Euler Finite Difference (BEFD)

This scheme approximates the time and space derivatives with a finite difference and uses an implicit method to guarantee convergence even for large time steps [7].

$$\begin{cases}\frac{\hat{\phi}-\phi^n}{\delta t} = \frac{1}{2}\Delta\hat{\phi} - V\hat{\phi} - \beta|\phi^n|^2\hat{\phi} + \Omega L_z\hat{\phi}\\ \phi^{n+1} = \frac{\hat{\phi}}{||\hat{\phi}||_0}\end{cases} \tag{12}$$

Hereafter, the formulation of the problem is presented for the 2D case. The 1D and 3D cases may be inferred analogously. We consider a box $\mathcal{O} =]-a_x, a_x[\times]-a_y, a_y[$ discretized in a grid $\mathcal{D}_{J,K} = \{(j,k) \in \mathbb{N}^2 : 1 \le j \le J-1\ 1 \le k \le K-1\}$ and the discretization steps $h_x = x_j - x_{j-1} = \frac{2a_x}{J}$, $h_y = y_k - y_{k-1} = \frac{2a_y}{K}$. The box is considered big enough so that Dirichlet boundary conditions may be imposed, i.e. $\phi(\vec{x}) = 0$ for $\vec{x} \in \partial\mathcal{D}_{J,K}$. The derivatives δ_x, δ_x^2 are given by

$$\delta_x\phi^n_{(j,k)} = \frac{\phi^n_{(j+1,k)} - \phi^n_{(j-1,k)}}{2h_x}$$

$$\delta_x^2\phi^n_{(j,k)} = \frac{\phi^n_{(j+1,k)} - 2\phi^n_{(j,k)} + \phi^n_{(j-1,k)}}{h_x^2}$$

δ_y, δ_y^2 are calculated likewise. Therefore, the discretized operators are expressed as:

$$L_z\phi^n_{(j,k)} = -i(x_j\delta_y\phi^n_{(j,k)} - y_k\delta_x\phi^n_{(j,k)}), \quad \Delta\phi^n_{(j,k)} = \delta_x^2\phi^n_{(j,k)} + \delta_y^2\phi^n_{(j,k)}$$

The scheme solves the linear system

$$\begin{cases}A\hat{\phi} = b^n\\ \phi^{n+1} = \frac{\hat{\phi}}{||\hat{\phi}||_0}\end{cases} \tag{13}$$

where $A = \frac{1}{\delta t}I - \frac{1}{2}\Delta + V + \beta|\phi^n|^2 - \Omega L_z$, and $b^n = \frac{\phi^n}{\delta t}$

B. Backward Euler pseudoSPectral (BESP)

This scheme uses Fourier methods in order to calculate the derivatives in the backward Euler scheme. We present the 1D version, with the discrete sine transform, as explained in [3] (artificial periodic boundary conditions are considered).

$$\begin{cases}\frac{\hat{\phi}-\phi^n}{\delta t} = \frac{1}{2}\Delta\hat{\phi} - V\hat{\phi} - \beta|\phi^n|^2\hat{\phi}\\ \phi^{n+1} = \frac{\hat{\phi}}{||\hat{\phi}||_0}\end{cases} \tag{14}$$

We define the discrete sine transform of a wavefunction:

$$\psi_l = \frac{2}{b-a}\int_a^b \phi(x)\sin(\mu_l(x-a))dx \approx \sum_{l=1}^{M-1}\phi\sin\left(\frac{jl\pi}{M}\right)$$

By using the sine transform, the second derivative of a function u can be computed as such:

$$D^s_{xx}u|_{x=x_j} = -\sum_{l=1}^{M-1}\mu_l^2\tilde{u_l}\sin(\mu_l(x_j-a)) \tag{15}$$

From the numerical scheme we presented, we can see that at each iteration we have to solve a nonlinear system. Here we present a way to solve it iteratively.

$$\frac{\phi_j^{(1),m+1} - \phi_j^n}{\tau} = \frac{1}{2}D^s_{xx}\phi^{(1),m+1}|_{x=x_j} - \alpha\phi_j^{(1),m+1} + (\alpha - V(x_j) - \beta|\phi_j^n|^2)\phi_j^{(1),m} \tag{16}$$

where $m \ge 0$, $\phi_j^{(1),0} = \phi_j^n$ and α is an stabilization parameter to make the numerical scheme go faster. Taking the sine transform of both sides of the equation:

$$\frac{\widetilde{(\phi^{(1),m+1})_l} - \widetilde{(\phi^n)_l}}{\tau} = -(\alpha + \frac{1}{2}\mu_l^2)\widetilde{(\phi^{(1),m+1})_l} + \widetilde{(G^m)_l} \tag{17}$$

where

$$G_j^m = (\alpha - V(x_j) - \beta|\phi_j^n|^2)\phi_j^{(1),m} \tag{18}$$

The recurrence relation in Fourier space is then:

$$\widetilde{(\phi^{(1),m+1})_l} = \frac{2}{2+\tau(2\alpha+\mu_l^2)}(\widetilde{(\phi^n)_l} + \tau\widetilde{((G^m))_l}) \tag{19}$$

By taking the inverse sine transform of the solution of the recurrence relation, we obtain the solution of the nonlinear system.

C. Other Methods (BESP with preconditioners)

The methods presented above are robust for the non-rotating case, with a low number of particles and non-strong interactions (i.e. $\beta < 500$). However, convergence is either very slow or not guaranteed for other cases, such as $\Omega > 0$. Thereof, fast and robust numerical methods can be applied, by linearizing the CNGF equation as in equation 13. However, the operators using derivatives (laplacian and angular momentum) are not calculated explicitly, but rather, we compute their image as in BESP, using FFT and IFFT to evaluate them. Therefore, we cannot have an explicit representation of A, but given $\boldsymbol{\phi}$ we may know $A(\boldsymbol{\phi})$. To solve a linear system in cases where A is unknown, but its image is known, iterative Krylov methods can be used. Additionally, preconditioners to the linear system can be used to accelerate the computation, such as the Thomas-Fermi preconditioner, $P^n = (\mathbb{I}/\delta t + \mathbb{V} + \beta|\boldsymbol{\phi^n}|^2)^{-1}$, yielding $(\mathbb{I} - P^nA^n)\boldsymbol{\phi^{n+1}} = P^nb^n$. This system can be computed efficiently through a Krylov method called BiCGStab, as shown in [2]. The stopping criteria for **all** methods above is $\max_{(x_j,y_k)\in\mathcal{D}}||\phi^{n+1}(x_j,y_k) - \phi^n(x_j,y_k)|| < \epsilon$

III. NUMERICAL RESULTS

In this section we present the numerical results of the simulations. We have used BEFD in 1D and 2D and BESP in 1D. The comparisons correspond to GPELab simulations and the known theoretical limits. In the simulations below, we have taken $= 10^{-6}\delta t$.

A. Quantum Harmonic oscillator limit

If we impose that $\beta = 0$ there is no inter-particle interaction and we recover the Quantum Harmonic Oscillator with ground state $\psi(r) \propto e^{-r^2/r_0^2}$ with $r_0 = \sqrt{2\hbar/m\omega}$. If the oscillator is dimensionless it can be shown that $r_0 = \sqrt{2}$, leading to $\psi(r) \propto e^{-r^2/2}$. In our model we have run the numerical methods with a discretization of 1024 points, dt = 0.01, and $\beta = 0$. We have fitted the data to a Gaussian profile $y = ae^{-bx^2}$. The BEFD scheme obtained more accurate

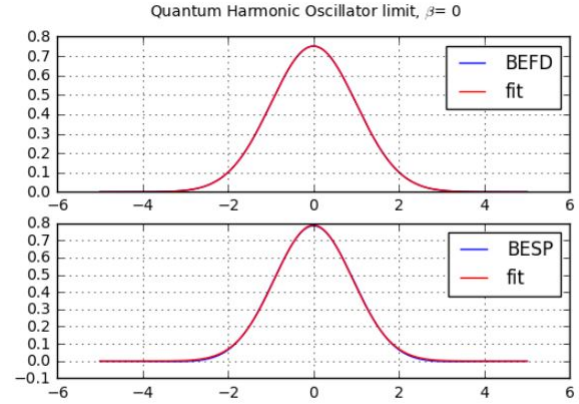

FIG. 1: Fit of the Harmonic approximation in the Harmonic limit, $\beta = 0$

results, with $b = 0.5001 \approx \frac{1}{2}$ while the BESP obtained $b = 0.6046$, a significant deviation from the expected result. We can also observe that the numerical error in BEFD is smaller than the numerical error of BESP. The parameters of BEFD have an error of the order of 10^{-8}, while the BESP parameters have an error of the order of 10^{-4}. Additionally, the GPELab results are also in accordance with the theoretical expectations.

B. Thomas-Fermi limit

If we impose a repulsive interaction with a high $\beta = 100$ we obtain the Thomas-Fermi approximation, which neglects the kinetic energy of the atoms and has the closed solution.

$$\psi(r) = \sqrt{\frac{\mu - m\omega^2 x^2/2}{gN}} \quad \text{where} \quad g = \frac{4\pi\hbar^2}{m}a. \tag{20}$$

We write the expression for the square of the wave, $\psi(x)^2 = \frac{\mu - m\omega^2 x^2/2}{gN}$. We will fit our numerical estimate of ϕ^2, using 1024 points dt = 0.001 for BESP and dt = 0.01 for BEFD, to a second order polynomial $\phi^2 = c_0x^2 + c_1x + c_2$. We don't know the theoretical coefficients *a priori*, since we are working with adimensional variables. However, the shape of the function will be the same, we expect the coefficient c_1 to be null. We also know that $\beta \propto \frac{Na}{a_0} \propto Ng$ so we expect the coefficients c_0 and c_2 to behave as $c_0 \propto \frac{1}{\beta}$, $c_2 \propto \frac{1}{\beta}$.

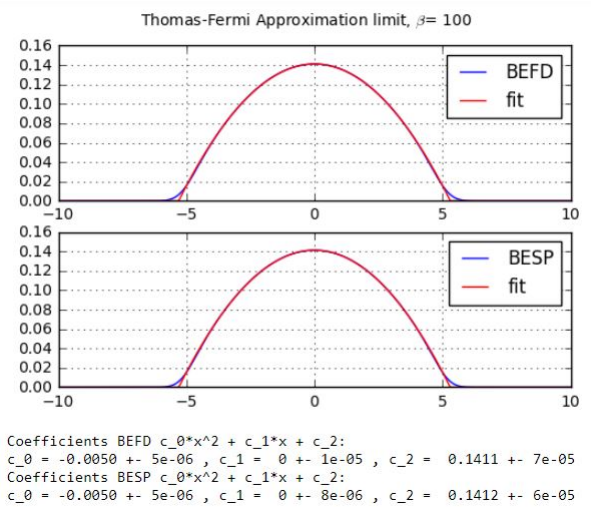

FIG. 2: Fit of the Thomas-Fermi approximation to ϕ^2 for $\beta = 100$

β	c_0 BEFD	c_2 BEFD	c_0 BESP	c_2 BESP
100	-0.0050	0.1411	-0.0050	0.1412
150	-0.0033	0.1233	-0.0034	0.1234
200	-0.0025	0.1120	-0.0025	0.1121
250	-0.0020	0.1040	-0.0020	0.1041
300	-0.0017	0.0979	-0.0017	0.0979

TABLE I: Dependence of Thomas-Fermi parameters with respect to β

In Table I we show the dependence of the coefficients with respect β. A linear regression of the dependence of c_0 and c_2 for the BEFD with respect $1/\beta$ has been done: $c0 = -0.47\frac{1}{\beta} - 0.0002$, and $c_2 = 6.39\frac{1}{\beta} + 0.0786$. We obtain a really good fit, with $R^2 = 0.989$. In both coefficients the slope is bigger than the y-intercept, but we must be careful because $1/\beta$ is small, in order to neglect the y-intercept in a linear regression $y = mx + n$ we need $\frac{n}{m*x} \approx 0$. For c_0 we have $\frac{-0.002}{-0.47*1/300} = 0.128 \approx 0$ but for c_2, $\frac{-0.0786}{6.39*1/300} = 3.69$. We can only consider that $c_0 \propto \frac{1}{\beta}$. If β was small we could also consider that $c_2 \propto \frac{1}{\beta}$ but making beta small invalidates the Thomas-Fermi limit. This result is coherent with the fact that $c_2 \propto \frac{\mu}{\beta}$, where μ is the chemical potential. The chemical potential can be thought as a energy per particle in the system and it should depend both on the interaction energy, proportional to β, and the potential V. c_2 can have a more complex dependence on β. Note that BEFD and BESP algorithms give the same results in the Thomas-Fermi limit.

C. Comparison with GPLab toolbox

To confirm the validity of the results, we also compared the results of the numerical algorithms we programmed with those provided by the GPELab toolbox presented in [1]. In Figure 3 we show the ground state solutions found by the two algorithms we coded and the one found by a BESP solver of GPELab, for an intermediate value of β. We can see that the solution found by GPELab is almost identical to the one

found by our Euler method and only slightly different to the one found by our BESP method.

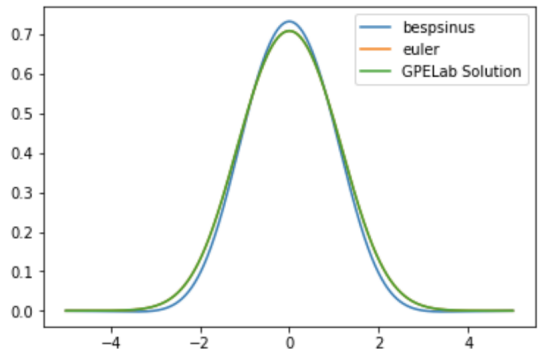

FIG. 3: Comparison of our results with those of GPELab for $\beta = 1$ with 1024 points and dt = 0.01

D. 2D-simulations

In this section we show the numerical results obtained in the BEFD 2D simulations. We use a potential

$$V(\mathbf{x}) = \frac{1}{2}(\gamma_x^2 x^2 + \gamma_y^2 y^2) + w_0 e^{-((x-x_0)^2+(y-y_0)^2)/d}$$

This potential is a harmonic potential with a perturbation corresponding to a far-blue detuned Gaussian laser beam (toroidal trap). We use a grid of 30 x 30 points and dt = 0.1 . We set $\Omega = 0$, $\beta = 1$. With our python code we show the level lines of both the potential and the ground state for different parameters.

Figure 4 shows the effect of changing the shape of the harmonic potential, at the left we have $\gamma_x = \gamma_y = 1$ and at the right the $\gamma_x = 3$, $\gamma_y = 1$. The wave-function gets squeezed in the x-axis because the bosons try to avoid the higher potential growth in the x-axis. Figure 5 shows the effect of the toroidal trap, plotting the level lines of both the potential and the ground state wave-function and the 3D plot of the wave-function. The result is a volcano shaped wave-function, the particles avoid the center because it has a higher potential and the higher density is accomplished at an external ring.

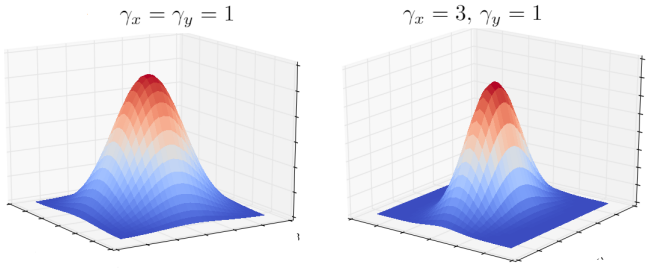

FIG. 4: 3D plot of the ground state for $\gamma_x = \gamma_y = 1$ (left) and $\gamma_x = 3$, $\gamma_y = 1$ (right),both with $w_0 = 0$

E. Brief Stability and Error Analysis

We have analyzed the effect of the time discretization parameter $\delta t = 1,\ 0.1,\ 0.01,\ 0.001$ in the 1D problem under different values of $\beta = 0,\ 20,\ 200$. In the BESP method we have seen that if the timestep δt is not small enough, there won't be convergence to the ground state. For $\beta = 0$ we needed $\delta t < 0.1$, for $\beta = 20$ we needed $\delta t < 0.01$ and for $\beta = 200$ we needed $\delta t < 0.001$. In BEFD all the chosen timesteps guaranteed convergence. In both BESP and BEFD the norm between two solutions, with δt different by an order of 10 and assuring convergence, was of the order of 10^{-5}. If we find a δt where there is convergence we don't need to increase δt to increase accuracy.

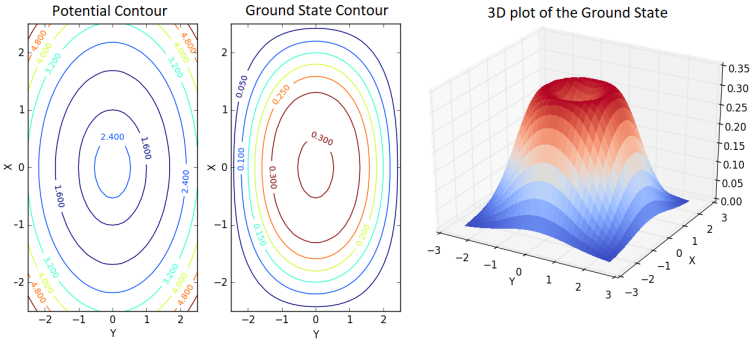

FIG. 5: Potential level lines (left), Ground State level lines (middle), 3D plot of the Ground State (right) for $\gamma_x = \gamma_y = 1$, $w_0 = 3$, $d = 1$

The runtime of the algorithms have also been analyzed. The average time of an iteration of BESP $t_{BESP} = 8.5 \cdot 10^{-4} s$ and BEFD $t_{BEFD} = 0.15 s$. We also observe that decreasing the parameter δt by a factor of 10 usually leads to an increase by a factor of 10 in the number of iterations. For a $\delta t = 1$ BEFD needs around 50 iterations and $\tau_{BEFD} \approx 7.6 s$. For a $\delta t = 0.01$ BESP needs around 500 iterations and $\tau_{BESP} \approx 0.43 s$. If β is bigger we will need $\delta t = 0.001$ and $\tau_{BESP} \approx 4.3 s$. BESP is a faster algorithm but we must be careful with the stability.

We have also studied the difference between the BESP and BEFD solutions. We have found that $||\phi_{BESP\beta=0} - \phi_{BEFD\beta=0}|| = 6.8 \cdot 10^{-2}$, $||\phi_{BESP\beta=20} - \phi_{BEFD\beta=20}|| = 1.9 \cdot 10^{-2}$ and $||\phi_{BESP\beta=200} - \phi_{BEFD\beta=200}|| = 2.8 \cdot 10^{-3}$. The difference between the two solutions gets smaller as we increase β.

IV. CONCLUSIONS

Solving the Schrödinger equation for a BEC boils down to solving a PDE numerically. The methods BEFD and BESP are compared, for different realistic potentials, in the 1D and 2D cases. Both methods yield an expected result for known cases in 1D: both are accurate in the T.F. limit. The BESP, as implemented hereof, yields to unaccurate results in the harmonic limit; however, in both cases BESP converges faster, and BEFD is more robust for variations of δt. As for the 2D case, results for the BEFD show the effect of having a toroidal trap. The discretization of the derivatives in the numerical method conditions its limitations; simple point-wise derivatives result in accurate ground-state solutions for low-particle BCEs, whereas using FFTs is suitable in more demanding cases, with rotational velocity or high values of β, where vortexes are found.

REFERENCES

[1] Xavier Antoine and Romain Duboscq. "GPELab, a Matlab toolbox to solve Gross-Pitaevskii equations I: Computation of stationary solutions". In: *Computer Physics Communications* 185 (11 2014), pp. 2969–2991.

[2] Xavier Antoine and Romain Duboscq. "Robust and Efficient Preconditioned Krylov Spectral Solvers for Computing the Ground States of Fast Rotating and Strongly Interacting Bose-Einstein Condensates." In: *Journal of Computational Physics* 258(1) (2014), pp. 509–523.

[3] Weizhu Bao and Yongyong Cai. "Mathematical Theory and Numerical Methods for Bose-Einstein Condensation". In: *AIMS* 6 (2013), pp. 1–135.

[4] Weizhu Bao and Qiang Du. "Computing the ground state solution of Bose-Einstein condensates by a normalized gradient flow". In: *SIAM J. Sci. Comput.* 25 (2004), pp. 1674–1697.

[5] Franco Dalfovo, Stefano Giorgini, Lev P. Pitaevskii and Sandro Stringari. "Theory of Bose-Einstein condensation in trapped gases." In: *Rev. Mod. Phys.* 71 (1999), p. 463.

[6] J. Rogel-Salazar. "The Gross-Pitaevskii Equation and Bose-Einstein condensates". In: *Eur. J. Phys.* 34 (2013), p. 247.

[7] Xavier Antoine, Christophe, Besse, Romain Duboscq, Vittorio Rispoli. "Acceleration of the imaginary time method for spectrally computing the stationary states of Gross-Pitaevskii equations." In: *Computer Physics Communications, Elsevier* 219 (2017), pp. 70–78.